

# The Entner–Doudoroff pathway empowers *Pseudomonas putida* KT2440 with a high tolerance to oxidative stress

Max Chavarría,<sup>1,2†</sup> Pablo I. Nikel,<sup>1†</sup>  
Danilo Pérez-Pantoja<sup>1</sup> and Víctor de Lorenzo<sup>1\*</sup>

<sup>1</sup>Systems and Synthetic Biology Program, Centro Nacional de Biotecnología (CNB-CSIC), 28049 Madrid, Spain.

<sup>2</sup>Escuela de Química, Universidad de Costa Rica, 2060 San José, Costa Rica.

## Summary

Glucose catabolism of *Pseudomonas putida* is carried out exclusively through the Entner–Doudoroff (ED) pathway due to the absence of 6-phosphofructokinase. In order to activate the Embden–Meyerhof–Parnas (EMP) route we transferred the *pfkA* gene from *Escherichia coli* to a *P. putida* wild-type strain as well as to an *eda* mutant, i.e. lacking 2-keto-3-deoxy-6-phosphogluconate aldolase. PfkA<sup>*E. coli*</sup> failed to redirect the carbon flow from the ED route towards the EMP pathway, suggesting that ED was essential for sugar catabolism. The presence of PfkA<sup>*E. coli*</sup> was detrimental for growth, which could be traced to the reduction of ATP and NAD(P)H pools along with alteration of the NAD(P)H/NADP<sup>+</sup> ratio. *Pseudomonas putida* cells carrying PfkA<sup>*E. coli*</sup> became highly sensitive to diamide and hydrogen peroxide, the response to which is very demanding of NADPH. The inhibitory effect of PfkA<sup>*E. coli*</sup> could in part be relieved by methionine, the synthesis of which relies much on NADPH. These results expose the role of the ED pathway for generating the redox currency (NADPH) that is required for counteracting oxidative stress. It is thus likely that environmental bacteria that favour the ED pathway over the EMP pathway do so in order to gear their aerobic metabolism to endure oxidative-related insults.

## Introduction

Glycolysis is the process run by nearly all organisms for the transformation of glucose and other monosaccharides into pyruvate (Romano and Conway, 1996; Bar-Even *et al.*, 2012). The wide occurrence of the process suggests that it is one of the earliest pathways that evolved for the production of energy (ATP) and reducing power [NAD(P)H], let alone generation of various building blocks for a plethora of cellular functions. The archetypal glycolysis is the so-called Embden–Meyerhof–Parnas (EMP) pathway (Romano and Conway, 1996), but other alternative routes [e.g. the Entner–Doudoroff (ED) pathway (Entner and Doudoroff, 1952; Conway, 1992; Romano and Conway, 1996)] also convert glucose into pyruvate. The EMP and ED pathways result in distinct yields of ATP, NAD(P)H and a range of different metabolic intermediates per molecule of sugar consumed (Neidhardt *et al.*, 1990). It is remarkable that while some microorganisms possess complete and coexisting EMP and ED pathways, others have one or the other, and finally there are bacteria that have one full route of one type and only a partial counterpart of the other (Fuhrer *et al.*, 2005). The obvious question is what determines the selection of such combinations and what are the evolutionary advantages for the bacteria that host them.

Inspection of the genome of the soil bacterium *Pseudomonas putida* KT2440 reveals that it encodes all the enzymes of the canonical ED pathway and the pentose phosphate (PP) route for metabolism of carbohydrates (Velázquez *et al.*, 2004; Nogales *et al.*, 2008; Puchałka *et al.*, 2008; Sohn *et al.*, 2010). In addition, the genome encodes a number of typically glycolytic (EMP) enzymes (Fig. 1). However, the downwards itinerary of glucose towards pyruvate cannot be completed because *P. putida* lacks the key glycolytic enzyme 6-phosphofructokinase (PFK; Velázquez *et al.*, 2004; Nogales *et al.*, 2008; Puchałka *et al.*, 2008). This activity catalyses the irreversible transformation of fructose-6-phosphate (F6P) to fructose-1,6-bisphosphate (FBP) by transferring a phosphate group from ATP or pyrophosphate to the C1 position of F6P (Ronimus and Morgan, 2001). PFK is commonly found in anaerobic and facultative anaerobic

Received 17 September, 2012; revised 3 December, 2012; accepted 3 December, 2012. \*For correspondence. E-mail vdlorenzo@cnb.csic.es; Tel. (+34) 91 585 4536; Fax (+34) 91 585 4506. †Ex aequo contribution.

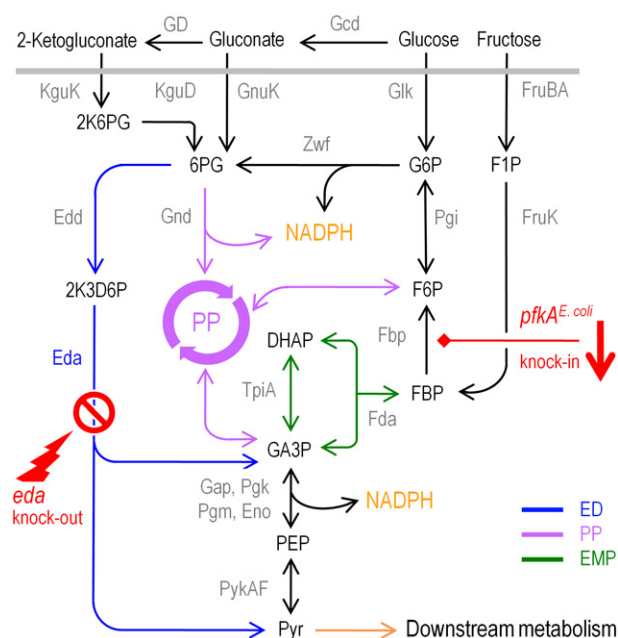


**Fig. 1.** Upstream central carbon metabolism in *P. putida* KT2440. Central carbon metabolism in *P. putida* KT2440 comprises the Entner–Doudoroff pathway (ED, blue), the pentose phosphate pathway (PP, purple) and an incomplete Embden–Meyerhof–Parnas pathway (EMP, green). The sketch summarizes: (i) the network of reactions in cells growing on glucose and fructose, highlighting the steps that generate NADPH, (ii) the heterologous reaction catalysed by 6-phosphofructokinase (*PfkA<sup>E. coli</sup>*) and (iii) the route blocked via inactivation of *eda*. The metabolites involved in each of the corresponding transformations are abbreviated as follows: G6P, glucose-6-phosphate; F1P, fructose-1-phosphate; FBP, fructose-1,6-bisphosphate; F6P, fructose-6-phosphate; 6PG, 6-phosphogluconate; 2K6PG, 2-ketogluconate-6-phosphate; 2K3D6P, 2-keto-3-deoxy-6-phosphogluconate; GA3P, glyceraldehyde-3-phosphate; DHAP, dihydroxyacetone phosphate; PEP, phosphoenolpyruvate; Pyr, pyruvate. The enzyme(s) that catalyse(s) each of the transformations is(are) termed as follows: Gcd, glucose dehydrogenase; GD, gluconate 2-dehydrogenase; FruBA, permease/phosphotransferase system for fructose; FruK, 1-phosphofructokinase; Glk, glucokinase; GnuK, gluconokinase; KguD, 2-ketogluconate-6-phosphate reductase; KguK, 2-ketogluconate kinase; Pgi, glucose-6-phosphate isomerase; Fbp, fructose-1,6-bisphosphatase; Fda, fructose-1,6-bisphosphate aldolase; Zwf, glucose-6-phosphate 1-dehydrogenase; Edd, 6-phosphogluconate dehydratase; Eda, 2-keto-3-deoxy-6-phosphogluconate aldolase; Gnd, 6-phosphogluconate dehydrogenase; TpiA, triosephosphate isomerase; Gap, glyceraldehyde-3-phosphate dehydrogenase; Pgm, phosphoglycerate kinase; Pgm, phosphoglycerate mutase; Eno, phosphoenolpyruvate hydratase; and PykAF, pyruvate kinase.

microorganisms (Hofmann, 1976; Ronimus and Morgan, 2001), as substrate level phosphorylation is the only way used by the cells to generate ATP in the absence of the oxygen-driven oxidative phosphorylation. For instance, *Escherichia coli* possesses two PFK isozymes (*PfkA* and *PfkB*), and this activity has been deemed essential for growth on glucose (Kim and Copley, 2007). Yet, the same enzyme is often missing in aerobic organisms (Fig. S1).

Because of the lack of such a PFK activity in *P. putida*, this microorganism consumes glucose almost exclusively through the ED pathway (Fuhrer *et al.*, 2005; del Castillo *et al.*, 2007; Chavarría *et al.*, 2012a). This intriguing metabolic feature was detected in very early studies on the biochemistry of this bacterium (De Ley, 1960; Vicente and Cánovas, 1973a; Latour and Lemanceau, 1997; Schleissner *et al.*, 1997), and also demonstrated through experiments of radiolabelling and metabolic flux analysis (Vicente and Cánovas, 1973b; Fuhrer *et al.*, 2005; Chavarría *et al.*, 2012a). In contrast, fructose can enter the partial glycolytic route present in *P. putida* as FBP through the action of the products of the *frubKA* gene cluster (Velázquez *et al.*, 2004; Chavarría *et al.*, 2011; 2012a,b). However, despite such a straightforward gate of fructose into central metabolism, this sugar is catabolized mostly through the ED pathway (~ 52%), with lesser contributions of the EMP pathway (~ 34%) and the PP pathway (~ 14%; Chavarría *et al.*, 2012a). The state of affairs is therefore not only that glucose necessarily enters into the ED pathway, but also that even when there is a choice for some sugars (e.g. fructose) between the ED and the EMP routes, *P. putida* favours the first over the second. The issue at stake is whether this peculiar metabolic configuration is just the result of an accidental evolutionary drift or it makes sense from the point of view of the bacterium environmental lifestyle.

The work below describes our attempts to shed some light on the predominance of the ED pathway for sugar metabolism in *P. putida*. Our approach involved the reconstruction *in vivo* of the complete set of enzymes for enabling a *bona fide* EMP glycolytic pathway in this bacterium in the presence or absence of a functional ED route. The resulting growth phenotypes, the energy status and the redox balance of the thereby engineered strains revealed not only that *P. putida* is altogether unable of redirecting C fluxes through the EMP pathway, but also that the functioning of a vigorous ED pathway is required for generation of the NADPH needed to endure oxidative conditions. These results highlight the connection between the central metabolism of *P. putida* and the environmental niches, often dominated by endogenous and exogenous oxidative stress, where this bacterium thrives.

## Results

### Habilitation of a complete EMP glycolytic pathway in *P. putida* KT2440

Figure 1 shows a reconstruction of the upstream processing of glucose and fructose by *P. putida* KT2440 with an indication of enzymes/genes that belong to the ED pathway, the EMP route and the PP pathway as derived from genomic annotations (Nelson *et al.*, 2002) and available metabolic models (Nogales *et al.*, 2008; Puchałka

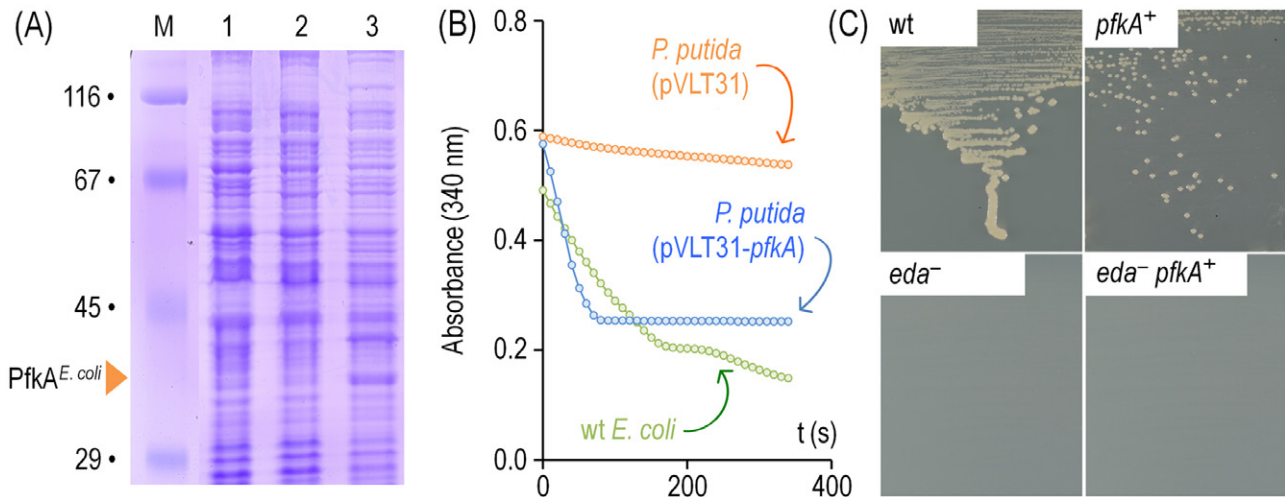


**Fig. 2.** Heterologous *pfkA<sup>E. coli</sup>* expression in *P. putida* KT2440.

A. SDS-PAGE stained with Coomassie Brilliant Blue showing the presence of PfkA from *E. coli* (34.8 kDa) in *P. putida* cells grown on LB medium. M, protein molecular weight marker; lane 1, cell-free extract from *P. putida* KT2440; lane 2, cell-free extract from *P. putida* KT2440 (pVLT31-*pfkA*) non-induced; and lane 3, cell-free extract from *P. putida* KT2440 (pVLT31-*pfkA*) induced with 0.5 mM IPTG.

B. Enzymatic assay for 6-phosphofructokinase assessed in cell-free extracts of wild-type *E. coli* W3110 (green), *P. putida* KT2440 carrying pVLT31 induced with 0.5 mM IPTG (orange) and *P. putida* KT2440 carrying pVLT31-*pfkA* induced with 0.5 mM IPTG (blue). All the strains were grown on LB medium and harvested during logarithmic growth ( $OD_{600} \sim 0.5\text{--}0.6$ ) for determinations. PFK activity (F6P + ATP  $\rightarrow$  FBP + ADP) was determined by coupling the ATP-dependent formation of FBP to the oxidation of NADH via fructose-1,6-bisphosphate aldolase, triosephosphate isomerase and glycerol-3-phosphate dehydrogenase (Steinbüchel, 1986). NADH oxidation was monitored by following the decrease in absorbance at 340 nm at 25°C. All the experiments were performed using 20  $\mu$ g of protein extract in a total volume of 200  $\mu$ l as described in *Experimental procedures*; a representative experiment is shown here. The specific PFK activities were 0.038 U  $mg^{-1}$  protein for *P. putida* KT2440 (pVLT31), 0.945 U  $mg^{-1}$  protein for *P. putida* KT2440 (pVLT31-*pfkA*) and 0.405 U  $mg^{-1}$  protein for *E. coli* W3110.

C. Growth experiments of *P. putida* KT2440 (wt), *P. putida* KT2440 carrying pVLT31-*pfkA* (*pfkA*<sup>+</sup>), *P. putida* KT2440 *eda*::mini-Tn5 (*eda*<sup>-</sup>) and *P. putida* KT2440 *eda*::mini-Tn5 carrying pVLT31-*pfkA* (*eda*<sup>-</sup> *pfkA*<sup>+</sup>). Cells were streaked onto solid M9 minimal medium containing 0.5 mM IPTG and 10 mM glucose as the only C source, and incubated at 30°C for 24 h.

*et al.*, 2008; Sohn *et al.*, 2010). A number of the enzymes indicated are encoded by two or more possible orthologues, the most conspicuous case being Zwf (glucose-6-phosphate 1-dehydrogenase), which corresponds to three possible alternative ORFs in the genome (PP1022, PP4042 and PP5351). Note that all of such pathways eventually converge in pyruvate as the port of entry to the downstream metabolism, but the biochemical itineraries are very different in each case (Figs 1 and S2). As mentioned above, the only missing enzyme to accomplish the entire set of activities for processing glucose through the EMP glycolytic pathway is PFK, which converts F6P into FBP. Inspection of such a metabolic map suggests that: (i) the mere knock-in of a heterologous PFK activity in *P. putida* would suffice to habilitate a functional EMP pathway in coexistence with a competing ED pathway and (ii) further knock-out of *edd* or *eda* genes would leave the EMP route as the only possible way of glucose catabolism. On this basis, we set out to express the *pfkA* gene of *E. coli* both into the wild-type *P. putida* strain and in its isogenic derivative lacking 2-keto-3-deoxy-6-phosphogluconate aldolase, generated through insertion of a mini-Tn5 transposon in the sole *eda* gene found in the genome of this bacterium. To this end, the *pfkA* sequence

was amplified from the genome of wild-type *E. coli* W3110 and cloned in the broad-host-range expression vector pVLT31 (de Lorenzo *et al.*, 1993), which allows conditional transcription of the inserted sequences upon addition of isopropyl-1-thio- $\beta$ -D-galactopyranoside (IPTG). Figure 2A shows that transformation of *P. putida* KT2440 with the thereby constructed plasmid (pVLT31-*pfkA*) resulted in the addition of a  $\sim 35$  kDa protein to the proteome of this bacterium. To test whether this operation originated a functional PFK activity in the new host, *P. putida* transformed either with the empty vector pVLT31 or with pVLT31-*pfkA* were grown on LB medium and induced with IPTG as explained in *Experimental procedures*. Soluble cell-free extracts of each of the cultures strains were then tested for PFK activity along with a positive control consisting of a cell-free extract of *E. coli* W3110 also grown on LB medium. The results of Fig. 2B show that *pfkA<sup>E. coli</sup>* expression in *P. putida* was translated into levels of PFK activity comparable to those observed in the wild-type *E. coli* strain. In particular, the specific PFK activities in the recombinants were 0.038 and 0.945 U  $mg^{-1}$  protein for *P. putida* KT2440 (pVLT31) and *P. putida* KT2440 (pVLT31-*pfkA*), respectively, and 0.405 U  $mg^{-1}$  protein for *E. coli* W3110.

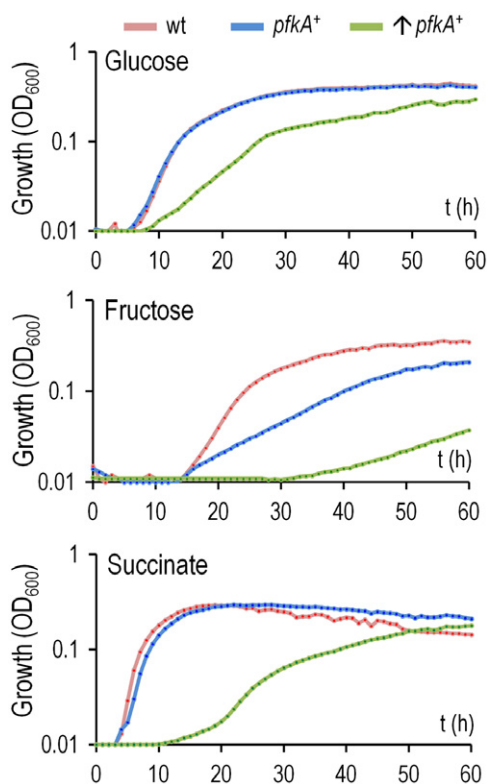


**Fig. 3.** Impact of the heterologous *pfkA<sup>E. coli</sup>* expression on the growth of *P. putida* KT2440 under both glycolytic and gluconeogenic regimes. Growth experiments were conducted with *P. putida* KT2440 carrying pVLT31 (vector, red), and *P. putida* KT2440 carrying pVLT31-*pfkA* in the absence (blue) and presence (green) of 0.5 mM IPTG in M9 minimal medium containing 10 mM of either glucose, fructose or succinate as the only C source. Growth was estimated by measuring the OD<sub>600</sub>, determined every 15 min over a 60 h period in microtitre plates. Results represent the average of five independent replicates from at least two independent cultures. Error bars (< 10% of the means) were omitted here for the sake of clarity.

In order to examine the effects of PfkA<sup>E. coli</sup> on the functioning of the metabolic circuit of Fig. 1, pVLT31-*pfkA* was also passed to the *eda::mini-Tn5* mutant and the complete set of strains tested for growth on M9 minimal medium plates with glucose as the only C source and IPTG to ensure *pfkA<sup>E. coli</sup>* expression. As shown in Fig. 2C (top panels), strain *P. putida* (pVLT31-*pfkA*) originated smaller colonies than the control bearing the insertless expression vector. This phenomenon was unexpected, as the current metabolic models (Nogales *et al.*, 2008; Puchalka *et al.*, 2008; Sohn *et al.*, 2010) predict that this enzyme should cooperate (at least partially) to the metabolism of hexoses, increasing the efficiency of processing these C sources (Baart *et al.*, 2010). On the other hand, PFK enters a considerable perturbation in the directionality of the fluxes that operate on cells growing on glucose (Fig. 1), which might be disadvantageous for growth. Still, the most surprising effect was that the pres-

ence of PfkA<sup>E. coli</sup> failed to revert the lack of growth of the *eda::mini-Tn5* mutant on glucose as the sole C source. This result was certainly not anticipated. While the lack of Eda should stop most of the metabolic flux of C from glucose towards pyruvate in the wild-type *P. putida* strain (the PP pathway being the only possible alternative route; Figs 1 and S2), the models predict that such a flux could be rerouted by PFK towards a canonical EMP pathway, i.e. glucose → G6P → F6P → FBP. That this was not the case suggested that the peculiar arrangement of the complete ED pathway and the partial EMP route (Fig. 1) is not just an accidental occurrence but a physiologically relevant feature of *P. putida*. The next experiments were devised to shed light on this question.

#### *PfkA<sup>E. coli</sup>* is detrimental for *P. putida* KT2440 growing under both glycolytic and gluconeogenic regimes

Inspection of Fig. 1 reveals the itineraries that glucose and fructose follow upon their processing through either the ED or EMP route as well as the upwards way that gluconeogenesis would have to go for building back metabolic intermediates from substrates such as succinate. The *a priori* prediction is that forcing conversion of F6P into FBP owing to a knocked-in PFK activity should affect fructose metabolism only minimally, because FBP is generated by the direct action of FruBKA on this sugar (Sawyer *et al.*, 1977; Chavarría *et al.*, 2012b), and all other intermediates could be reloaded through the reversible reactions within the network. On the other hand, succinate metabolism through the lower metabolic cycles (Romano and Conway, 1996) originates the two main gluconeogenic currencies, phosphoenolpyruvate and pyruvate. Again, according to the biochemical map of Fig. 1, this should suffice to reload all the pools of intermediates even if PFK forces the non-native flux F6P → FBP. In order to test these possible physiological scenarios, we compared the growth of *P. putida* KT2440 (pVLT31-*pfkA*) on M9 minimal medium with glucose, fructose or succinate as the sole C source, along with the control strain transformed with the insertless vector. As shown in Fig. 3, expression of PFK slowed growth in all the three cases. The impact on growth can be qualitatively ordered as fructose >> glucose ~ succinate. The effect was more pronounced in the case of fructose; the mere presence of the pVLT31-*pfkA* plasmid restrained the growth of the strain very significantly, even in the absence of IPTG. The specific growth rates were also calculated for each condition (Table 1), and, as hinted by the growth curve plots, a stronger negative effect exerted by PfkA<sup>E. coli</sup> was observed on the growth of cells cultured on glycolytic C sources than in cells grown on succinate.

These unexpected results made us re-examine the reactions around the F6P node. Figure 1 shows that the

**Table 1.** Growth parameters in batch cultures of the different *P. putida* KT2440 recombinants under study.

<i>P. putida</i> KT2440	C source <sup>a</sup>	IPTG <sup>b</sup>	$\mu$ (h <sup>-1</sup> ) <sup>c</sup>
pVLT31	Glucose	–	0.36 ± 0.04
pVLT31– <i>pfkA</i>		–	0.35 ± 0.04
pVLT31– <i>pfkA</i>		+	0.13 ± 0.01
pVLT31	Fructose	–	0.24 ± 0.02
pVLT31– <i>pfkA</i>		–	0.09 ± 0.01
pVLT31– <i>pfkA</i>		+	0.05 ± 0.01
pVLT31	Succinate	–	0.49 ± 0.06
pVLT31– <i>pfkA</i>		–	0.49 ± 0.03
pVLT31– <i>pfkA</i>		+	0.15 ± 0.02

**a.** The specific growth rate was determined during logarithmic growth from the experimental data shown in Fig. 3. Cells were cultured on M9 minimal medium containing the corresponding C source at 10 mM and, when induced, 0.5 mM IPTG.

**b.** Addition of IPTG to cultures of the strains carrying pVLT31 did not translate into significant effects on the specific growth rate values.

**c.** Reported results represent the mean value ± standard deviation of quintuplicate measurements from at least two independent cultures.

most immediate effect of PFK on fructose metabolism should be a decrease of available F6P, G6P and ultimately 6-phosphogluconate (6PG). Since both F6P and 6PG are the main suppliers of carbon to the PP pathway, one option is that the inhibition caused by PfkA<sup>E. coli</sup> on *P. putida* grown on either glycolytic or gluconeogenic substrates is due to the dearth of cellular building blocks (e.g. pentoses) derived from the PP cycle (Sprenger, 1995). However, this possibility seems unlikely, as the flux of carbon through the PP pathway in glucose-grown cells was shown to be very low (Führer *et al.*, 2005; Chavarría *et al.*, 2012a). Nevertheless, in order to test this scenario we examined whether addition of ribose to the medium could rescue totally or partially the detrimental effect of PfkA<sup>E. coli</sup> on *P. putida* KT2440 (pVLT31–*pfkA*). Ribose enters directly into the PP pathway upon phosphorylation to ribose-5-phosphate (Meijnen *et al.*, 2012), and therefore it should reload that metabolic node with all the necessary C5 precursors of essential macromolecules [e.g. DNA and RNA (Neidhardt *et al.*, 1990)]. While *P. putida* KT2440 can grow well on ribose as the sole C source (albeit at a slow specific growth rate,  $\mu = 0.19 \pm 0.03$  h<sup>-1</sup>), *P. putida* KT2440 (pVLT31–*pfkA*) cultured on M9 minimal medium containing both glucose and ribose had no detectable differences in growth parameters, i.e. specific growth rate and final cell density, as compared with cultures amended with glucose alone (data not shown). Since the results of this experiment were not entirely conclusive (e.g. ribose transport and/or catabolism could be inhibited in the presence of glucose), we decided to explore other alternative explanations to the detrimental effects of PFK based not just on the lack of specific metabolites but on the effects of the outcome of the

*pfkA*<sup>E. coli</sup> knock-in on the primary biochemical functions of the cell, such as ATP production and generation of reducing equivalents.

#### *PfkA*<sup>E. coli</sup> decreases the energy status and alters the redox homeostasis of *P. putida* KT2440

In order to diagnose the reason(s) for the toxic effect of PFK in *P. putida* under various growth conditions, we first measured the intracellular concentration of ATP as a gross descriptor of the energy status of cells expressing or not *pfkA*<sup>E. coli</sup>. To this end, *P. putida* (pVLT31) and *P. putida* (pVLT31–*pfkA*) were grown on M9 minimal medium with glucose (with or without IPTG), samples were collected in the exponentially growing culture and ATP was determined with the luminescence-based protocol described in *Experimental procedures*. The results of Fig. 4A show that *pfkA*<sup>E. coli</sup> expression sharply decreased the intracellular contents of ATP with respect to cells

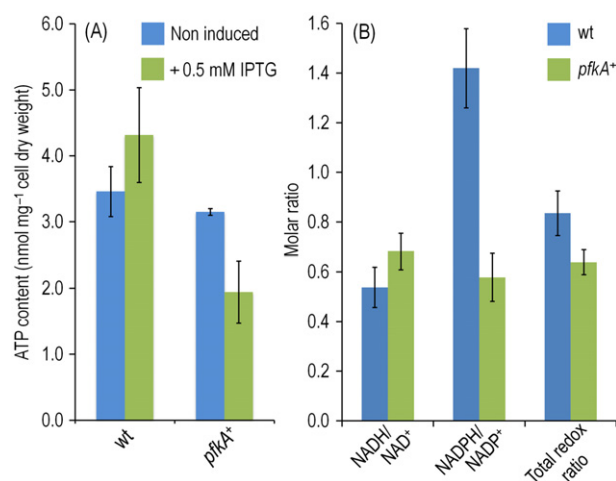


**Fig. 4.** Determination of intracellular ATP and pyridine nucleotide cofactors in *P. putida* KT2440 in the absence or presence of PfkA<sup>E. coli</sup>.

**A.** ATP determinations were performed in exponentially growing *P. putida* KT2440 cells (OD<sub>600</sub> ~ 0.5–0.6) carrying either pVLT31 (vector) or pVLT31–*pfkA* grown on M9 minimal medium containing 10 mM glucose as the sole C source in absence or presence of 0.5 mM IPTG (see *Experimental procedures* for further details). ATP concentrations were normalized to the cell dry weight of the culture sample used for the determination. Each bar represents the mean value of the ATP content ± standard deviation of duplicate measurements from at least three independent experiments.

**B.** Total and individual redox ratios were determined from the absolute intracellular concentrations of NAD<sup>+</sup>, NADH, NADP<sup>+</sup> and NADPH. All the pyridine nucleotide cofactors were determined enzymatically in exponentially growing *P. putida* KT2440 (OD<sub>600</sub> ~ 0.5–0.6) cells carrying either pVLT31 (vector) or pVLT31–*pfkA* grown on M9 minimal medium containing 10 mM glucose as the sole C source, 2 h after induction of *pfkA*<sup>E. coli</sup> expression by the addition of 0.5 mM IPTG. In all cases, each bar represents the mean value of the corresponding parameter ± standard deviation of duplicate measurements from at least two independent experiments.

lacking this activity or not induced with IPTG. While this drop in ATP levels would suffice to explain the negative effect of PFK on the growth of *P. putida* recombinants, its biochemical explanation is not trivial. On one hand, the step F6P → FBP catalysed by PfkA<sup>*E. coli*</sup> consumes one ATP equivalent per F6P molecule. But once the complete EMP route is enabled, the process would yield more ATP per mole of glucose consumed than the ED pathway (Fig. S2). Therefore, introduction of a PFK activity to rehabilitate the missing step in *P. putida* is predicted to ultimately increase, rather than decrease, the ATP pool. That this is not the case suggests that the pathway is not properly reconstructed and that the PFK reaction probably results in a futile drain of ATP. The lack of EMP-based glycolysis in *P. putida* may thus not be the result of an adventitious lack of PFK but a fundamental evolutionary trait that favours the alternative ED pathway in this microorganism.

Since the main physiological differences between the EMP and ED pathways are the overall yields of ATP (higher for the EMP pathway) and NAD(P)H (higher for the ED pathway), we wondered whether the reason for missing the EMP pathway was related to its lower ability to generate reducing power (Fig. S2). To test this hypothesis, the intracellular levels of both oxidized and reduced pools of nicotinamide dinucleotides were measured in isogenic, IPTG-induced *P. putida* (pVLT31) and *P. putida* (pVLT31-*pfkA*) grown under the same conditions as employed before for ATP determinations. The results shown in Fig. 4B indicate that cells expressing PfkA<sup>*E. coli*</sup> (and thus pulling down the flux of glucose towards FBP rather than channelling it through the ED and PP pathways) have a significantly altered redox homeostasis. Specifically, the total redox ratio dropped by c. 25% in cells expressing *pfkA<sup>E. coli</sup>* (Fig. 4B). The NADPH/NADP<sup>+</sup> ratio was much more affected by the activity of PfkA<sup>*E. coli*</sup> than the NADH/NAD<sup>+</sup> ratio, which remained essentially the same irrespective of the presence of PFK. This situation may stem from a poor functioning of either the ED pathway or the PP pathway. But since substrates of the PP pathway do not revert the toxic effects of PFK (see above) and considering that the flux of glucose through the PP pathway is known to be very low (Fuhrer *et al.*, 2005; Chavarría *et al.*, 2012a), it is most likely that the drop in reducing power availability stems from the perturbation that the PfkA<sup>*E. coli*</sup> knock-in propagates into the ED pathway. It is thus plausible that a second cause for PFK toxicity in the metabolic context of *P. putida* (apart of the ATP decrease) is the dramatic drop in NADPH availability caused by the diversion of the C flux naturally going towards the ED route into a non-productive direction. Since such a deficiency of reducing power has predictable phenotypic consequences (Blank *et al.*, 2008; Fuhrer and Sauer, 2009; Ebert *et al.*, 2011),

we set out to make the connection between the prevalence of the ED pathway in *P. putida* and some of its noticeable phenotypic traits.

#### *Pseudomonas putida* KT2440 expressing *pfkA<sup>E. coli</sup>* is hypersensitive to redox stress

In order to compare the endurance of *P. putida* KT2440 expressing or not *pfkA<sup>E. coli</sup>* with oxidative conditions, we adopted tolerance to diamide (DA) as a descriptor of changes in the intracellular redox status. DA is a membrane-permeable thiol-specific oxidizing agent, which reacts with both low molecular mass thiols and protein sulphhydryls (Bearson *et al.*, 2009; Pöther *et al.*, 2009). Among other effects, DA oxidizes glutathione and promotes the formation of disulfide bonds in the cytoplasm (Wax *et al.*, 1970; Kosower and Kosower, 1995). Bacteria counteract the resulting stress through the reduction of these intracellular disulfides by means of NADPH-dependent thioredoxins (Carmel-Harel and Storz, 2000; Cumming *et al.*, 2004). Tolerance/sensitivity to DA thus ultimately depends on the intracellular levels of NADPH (Butler *et al.*, 2002), and any drop in the concentration of this cofactor must result in an increased damage by DA. On this basis, the effect of DA on *P. putida* expressing or not *pfkA<sup>E. coli</sup>* was tested in respect to two kinetic parameters, growth retardation (i.e. the time span needed to start logarithmic growth) and normalized growth coefficients (i.e. the ratio between the specific growth rates observed in the presence and the absence of DA respectively). As shown in Fig. 5A, increasing the concentrations of DA resulted in longer growth retardation irrespective of the presence of the heterologous PFK, but, as anticipated, this effect was much more pronounced for the strain carrying PfkA<sup>*E. coli*</sup>. In fact, in the presence of 1 mM DA, *P. putida* KT2440 (pVLT31-*pfkA*) had a growth retardation approximately twofold longer than that of the control strain carrying the empty vector (Fig. 5A). Moreover, judging by the slope in the plots of growth retardation vs. DA concentration, the strain expressing *pfkA<sup>E. coli</sup>* became much more sensitive to DA at concentrations > 0.1 mM than the control strain. The redox perturbation caused by DA also propagated into differences in the normalized growth coefficients. Specific growth rates attained in the presence of DA were lower for all the experimental strains, but, again, *P. putida* KT2440 (pVLT31-*pfkA*) showed a more dramatic decrease in this parameter (Fig. 5B). When growing in the presence of 1 mM DA, the control strain had a normalized growth coefficient of 86.1 (i.e. a reduction of ~ 14% in the specific growth rate observed in the absence of DA). Under the same conditions, *P. putida* KT2440 (pVLT31-*pfkA*) had a normalized growth coefficient of 60.3 (i.e. a reduction of ~ 40% in the specific growth rate observed in the absence

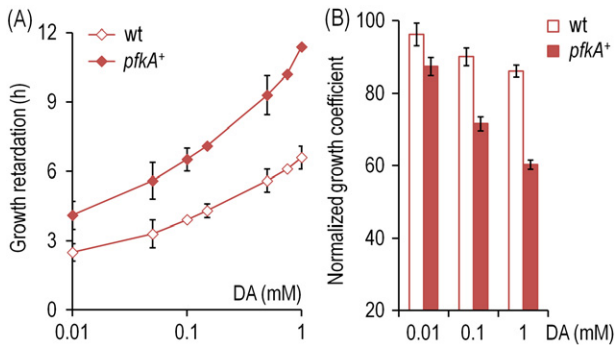


**Fig. 5.** Evaluation of the stress resistance in *P. putida* KT2440 treated with diamide in the absence or presence of PfkA<sup>E. coli</sup>. A. Growth retardation, i.e. the time span needed to start logarithmic growth (Dalgaard and Koutsoumanis, 2001), was determined in cultures of *P. putida* KT2440 (pVLT31, vector) or *P. putida* KT2440 (pVLT31-*pfkA*) grown on M9 minimal medium containing 10 mM glucose as the sole C source, 0.5 mM IPTG and the indicated concentration of diamide (DA). B. Normalized growth coefficients [i.e.  $100 \times (\mu_{\text{experimental}}/\mu_{\text{control}})$ , where  $\mu_{\text{experimental}}$  and  $\mu_{\text{control}}$  are the specific growth rates under stressful (DA added) and control (without added DA) conditions respectively] were calculated in cultures of *P. putida* KT2440 (pVLT31, vector) or *P. putida* KT2440 (pVLT31-*pfkA*) grown on M9 minimal medium containing 10 mM glucose as the sole C source, 0.5 mM IPTG and the indicated concentration of DA. Each data point or bar represents the mean value of the corresponding parameter  $\pm$  standard deviation of triplicate measurements from at least three independent experiments.

of DA). Taken together, these results document an increased sensitivity to DA in cells expressing the knocked-in glycolytic enzyme.

A second type of redox stress was brought about just by treating the same set of strains with hydrogen peroxide (H<sub>2</sub>O<sub>2</sub>). While the general oxidative damage caused by this agent affects proteins as well as lipids and DNA (Storz *et al.*, 1990; Demple, 1991), the mechanism for counteracting its action involves the sensing of the -SH vs. S-S ratio in intracellular glutathione and the expression of several catalases and peroxidases (Storz *et al.*, 1990; Demple, 1991; Izawa *et al.*, 1996; Blank *et al.*, 2010). These detoxifying processes ultimately depend on the NADPH availability (Storz *et al.*, 1990; Storz and Imlay, 1999; Carmel-Harel and Storz, 2000). As shown in Fig. 6, when cells of the recombinants were challenged with H<sub>2</sub>O<sub>2</sub> in soft-agar experiments, the growth inhibition zone detected resulted consistently larger for cells carrying pVLT31-*pfkA*. A slightly higher sensitivity was observed for *P. putida* (pVLT31-*pfkA*), as compared with the control strain carrying the empty vector, even in the absence of IPTG (top panels). An inhibition halo approximately twofold larger than that of the non-induced control was observed for the *pfkA*<sup>E. coli</sup> strain upon induction with IPTG.

Since *pfkA*<sup>E. coli</sup>-expressing cells become more sensitive to both DA and H<sub>2</sub>O<sub>2</sub>, we hypothesize that the major physiological consequence of perturbing the extant meta-

bolic network of *P. putida* with PFK is to increase its sensitivity to oxidative stress. But how is such a drop of NADPH translated into growth inhibition in the absence of any induced stress, as observed in Fig. 3?

#### Methionine relieves the inhibitory effect of *pfkA*<sup>E. coli</sup> expression in *P. putida* KT2440

Any multicomponent system subjected to a given stress succumbs to it when the activity or the concentration of an essential constituent becomes limiting even if the other elements are not affected (Ravasz *et al.*, 2002; Imlay, 2008). Anabolic processes depending on NADPH are thus predicted to be very sensitive to fluctuations of this cofactor. Inspection of the complete metabolic network of *P. putida* reveals that methionine biosynthesis is perhaps the most NADPH-consuming single metabolic route in this bacterium. As shown in Fig. 7A, up to 4 moles of NADPH are necessary to generate 1 mole of methionine from aspartate and inorganic sulfate. In fact, sulfur-containing amino acids require more NADPH to be synthesized *de novo* than other amino acids in several microorganisms (Neidhardt *et al.*, 1990; Sekowska *et al.*, 2000), and some of the enzymes involved in their formation have been shown to be very sensitive to oxidative stress (Benov *et al.*, 1996; Hondorp and Matthews, 2004). Shortage of the cofactor is therefore expected to create a functional auxotrophy or bradytrophism for methionine. To test whether this was the case, we evaluated the effects of adding methionine to DA-stressed cultures.

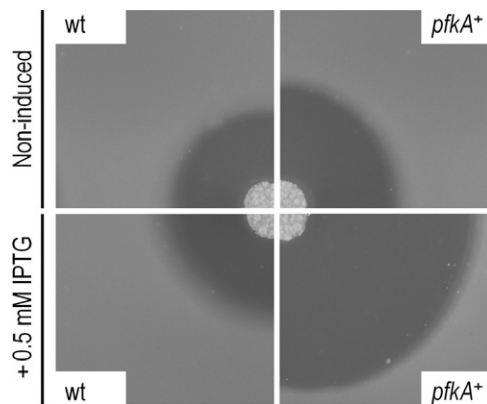


**Fig. 6.** Evaluation of the stress resistance in *P. putida* KT2440 treated with H<sub>2</sub>O<sub>2</sub> in the absence or presence of PfkA<sup>E. coli</sup>. Soft-agar assays were conducted by pouring a 0.75% (w/v) agar suspension [containing 1% (w/v) NaCl] of *P. putida* KT2440 (pVLT31, vector) or *P. putida* KT2440 (pVLT31-*pfkA*) onto M9 minimal medium plates containing 10 mM glucose as the sole C source, in the absence or presence of 0.5 mM IPTG. Filter discs (5 mm diameter) were placed onto the homogeneous bacterial lawn and soaked with 25  $\mu$ l of 30% (v/v) H<sub>2</sub>O<sub>2</sub>. The plates were incubated at 30°C during 24 h and photographed. Representative results from duplicated assays are shown.

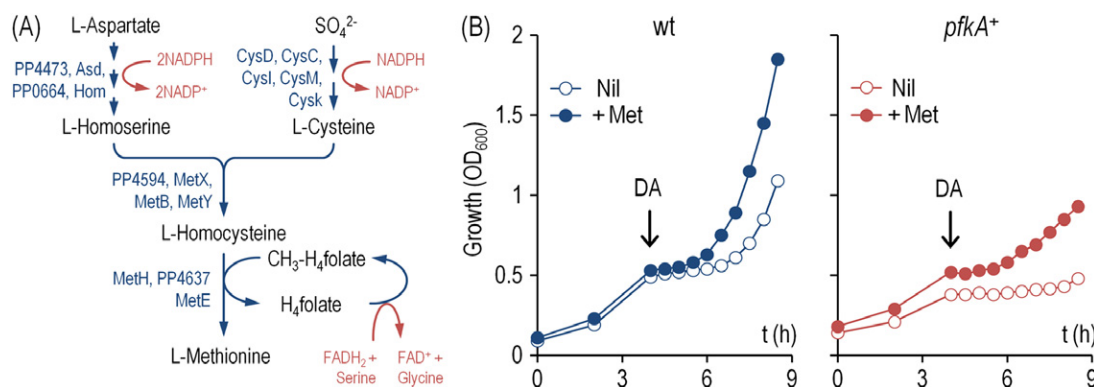


**Fig. 7.** Perturbation of the methionine metabolism in *P. putida* KT2440 treated with diamide in the absence or presence of PfkA<sup>E. coli</sup>. **A.** Simplified scheme of the main pathways involved in methionine synthesis from aspartate and inorganic sulfate in *P. putida* KT2440. Relevant enzymatic steps are identified by means of either the enzyme name or the corresponding locus (PP) number(s) as annotated by Nelson and colleagues (2002). CH<sub>3</sub>-H<sub>4</sub>folate and H<sub>4</sub>folate represent 5-methyltetrahydrofolate (i.e. levomefolate) and tetrahydrofolate, respectively, involved in the reaction catalysed by MetH, the methionine synthase isozyme dependent of vitamin B12. **B.** Methionine (Met)-dependent relief of the toxic effect caused by diamide (DA). *Pseudomonas putida* KT2440 (pVLT31, vector) or *P. putida* KT2440 (pVLT31-*pfkA*) was grown until mid-exponential phase (OD<sub>600</sub> ~ 0.5) on M9 minimal medium containing 10 mM glucose as the sole C source and 0.5 mM IPTG, with or without 50 μg ml<sup>-1</sup> methionine, and added with 1 mM DA (indicated with a vertical arrow). Growth was estimated by periodic measurements of the OD<sub>600</sub> to evaluate the ability of the cells to recover from the DA challenge. Results represent the average of three independent replicates from at least two independent cultures, and error bars (< 10% of the means) are not shown.

As shown in the preceding section, addition of DA to the culture medium does not kill the bacteria, but causes an almost-immediate growth arrest, the extent of which is dependent on the redox status of the cells. As such, cells are able to resume growth once redox homeostasis is properly restored. *Pseudomonas putida* KT2440 (pVLT31) and *P. putida* KT2440 (pVLT31-*pfkA*) were thus treated with 1 mM DA during exponential phase, and growth was monitored thereafter to evaluate the ability of the cells to recover from such an insult. As postulated, cultures amended with methionine successfully recovered from the oxidative challenge (Fig. 7B) when compared with cultures without the amino acid. This was indicative that methionine production is one of the first (if not the first) metabolic assets to fail under oxidative stress, most likely because of the dearth of NADPH originated by the cellular response to PfkA<sup>E. coli</sup> as discussed above. When the same experiment was repeated with cells expressing the knocked-in *pfkA<sup>E. coli</sup>* gene, the effect of methionine addition became more evident, as cells challenged with DA in the absence of the amino acid were altogether unable to recover thereafter. Thus, that methionine relieved the inhibition caused separately by DA and PFK and that the same amino acid could mitigate the increased sensitivity of cells expressing *pfkA<sup>E. coli</sup>* to the added stressor traced all these effects to the varying pools of NADPH under the conditions tested.

## Discussion

The data above demonstrate that knocking-in a heterologous and functional PFK in *P. putida* not only fails to

reconstruct a productive EMP pathway but it enters a major perturbation into its native metabolic network that is ultimately detrimental for growth. The perturbation in the central metabolism due to *pfkA<sup>E. coli</sup>* expression produces an imbalance in the ATP and NADPH levels (Fig. 4), which propagates into a significant growth inhibition even in the absence of any added stressor. While the drop in ATP levels caused by PFK expression suffices to explain the toxic effect it elicits, we argue that the concomitant decrease in NADPH is in fact what explains the preference of *P. putida* for the ED pathway. Why? While the logic of EMP glycolysis is geared towards production of energy (ATP) and building blocks for biomass production (Bar-Even *et al.*, 2012), the ED route is more proficient in generation of reducing power, in particular NADPH (Conway, 1992; Kim *et al.*, 2008). This cofactor has many metabolic functions, out of which synthesis of various amino acids (e.g. methionine) and counteracting oxidative stress predominate (Storz *et al.*, 1990; Storz and Imlay, 1999; Singh *et al.*, 2007; Ying, 2008). In line with this concept, biochemical processes very demanding in terms of NADPH availability [such as poly(3-hydroxybutyrate) accumulation in recombinant *E. coli*] are favoured by the addition of amino acids such as methionine and cysteine, the synthesis of which would otherwise consume high amounts of reducing equivalents (Nikel *et al.*, 2008a). A simple test with the sulfhydryl-oxidizing compound DA allowed us to visualize that *P. putida* is more resistant to redox stress than *E. coli* (Fig. S3). The data of this article consistently support the notion that the reason behind the prevalence of the ED route for glucose processing in *P. putida* (and many other microorganisms) and the



detrimental effect of knocking-in a PFK activity is no other but the high demand of NADPH needed to sustain the environmental lifestyle of this bacterium. Within this conceptual framework, it does not come as a surprise that both Edd and Eda are essential for growth of *P. putida* KT2440 on minimal medium (Molina-Henares *et al.*, 2010). PFK catalyses a reaction that drains G6P and F6P from the upper metabolic circuit shown in Fig. 1. These substrates feed the major NADPH-producing reactions, and their shortage would translate into a low NADPH availability. Since the activity of the PP route is only residual in glucose-grown cells (Fuhrer *et al.*, 2005; Chavarría *et al.*, 2012a), it is most plausible that most (if not all) of this effect can be traced to the malfunctioning of the ED pathway. Furthermore, since FBP necessarily generated by PFK appears unable to follow a productive EMP route, the knock-in of *pfkA<sup>E.coli</sup>* probably results in a futile ATP-hydrolysing cycle. Note, however, that the state of affairs just discussed for *P. putida* KT2440 might be specific for this genus. Expression of *pfkA<sup>E.coli</sup>* in *Cupriavidus necator* and *Xanthomonas oryzae*, which also have an ED route and lack a PFK activity, does result in an EMP metabolism of sorts (Steinbüchel, 1986; Jang *et al.*, 2012). In other microorganisms that lack a native EMP metabolism, such as *Gluconobacter oxydans*, the ED pathway seems to be dispensable and even unfavourable (Richhardt *et al.*, 2012). In contrast, we show above that the upper flux of carbon in *P. putida* cannot be redirected into the EMP pathway merely by knocking-in *PfkA<sup>E.coli</sup>* even in the case where the ED route is inactivated by the *eda* mutation (Fig. 1).

One way or the other, ED metabolism is far more widely distributed in nature than has been previously recognized, and the enzymes of this pathway are highly conserved (Conway, 1992; Peekhaus and Conway, 1998; Sato and Atomi, 2011; Fabris *et al.*, 2012). It is thus possible that microorganisms that solely have a vigorous ED pathway connected to the rest of the metabolic network in the fashion herein described are more prepared for dealing with both endogenous and exogenous oxidative stress than others (e.g. *E. coli*) that are adapted to perform EMP glycolysis (Loza-Tavera and de Lorenzo, 2011). This may not only account for the abundance of *Pseudomonas* strains in sites afflicted by a considerable physicochemical stress, but also provide an explanation as for why pseudomonads (and close phylogenetic relatives) are frequent hosts of biodegradative operons that encode strong oxidative enzymes (Ramos *et al.*, 2009; Sohn *et al.*, 2010; Fuchs *et al.*, 2011; Pérez-Pantoja *et al.*, 2012). In full agreement with these concepts, the ED pathway has been recently shown to be essential for infection in pathogens that have to quell oxidative stress during their intracellular lifestyle (Harada *et al.*, 2010; Patra *et al.*, 2012).

## Experimental procedures

### Bacterial strains, plasmids and DNA manipulation procedures

All *Pseudomonas* strains used in this work were derived from *P. putida* strain KT2440 (Bagdasarian *et al.*, 1981) and they are summarized in Table S1, along with other bacteria and plasmids used in this study. For the heterologous expression of PFK, the entire coding sequence of the *pfkA* gene from *E. coli* W3110 (963 bp) was amplified by PCR using oligonucleotides *pfkA*-F (5'-CGC GGG GTA CCA GGA AAG ATA TAA TGA TTA AGA AAA TCG GT-3') and *pfkA*-R (5'-CGC GGA AGC TTT TAA TAC AGA AAA AAC GCG CAG TC-3') and Vent<sub>R</sub><sup>TM</sup> DNA polymerase (New England BioLabs, Ipswich, MA, USA) by following standard procedures (Sambrook and Russell, 2001). The resulting DNA fragment was digested with KpnI and HindIII, ligated into the polylinker of the expression plasmid pVLT31 (de Lorenzo *et al.*, 1993) restricted with the same enzymes and subsequently transformed into *E. coli* CC118λ*pir*. This plasmid was isolated, the amplicon sequenced and finally electroporated into *P. putida* KT2440 and its *eda::mini-Tn5* derivative (Ducque *et al.*, 2007) as previously described (Choi *et al.*, 2006).

### Growth conditions and determination of kinetic parameters

All *P. putida* strains were aerobically grown batchwise at 30°C with shaking at 170 r.p.m. on either LB or M9 minimal medium (Miller, 1972; Sambrook and Russell, 2001) containing either 10 mM glucose, fructose or succinate as the sole C and energy source. Tetracycline was added at 10 µg ml<sup>-1</sup> to select for the strains carrying pVLT31 and pVLT31-*pfkA*. Whenever needed, media were solidified by addition of 1.5% (w/v) agar. Inocula were grown for 18 h on LB medium with 10 µg ml<sup>-1</sup> tetracycline. Cells were harvested by centrifugation (15 min, 4000 g, 4°C), washed twice with 10 mM MgSO<sub>4</sub> and finally resuspended in 10 mM MgSO<sub>4</sub> to an optical density measured at 600 nm (OD<sub>600</sub>) of ~ 3. Unless otherwise stated, cell suspensions were then diluted to an OD<sub>600</sub> of ~ 0.03 in M9 minimal medium containing the appropriate C source, 10 µg ml<sup>-1</sup> tetracycline, and in the presence or absence of 0.5 mM IPTG as required. Cultures used for *in vitro* determinations and stress studies with DA were developed in 250 ml Erlenmeyer flasks containing 50 ml of the corresponding culture medium. Samples used to analyse growth parameters were prepared by distributing 200 µl aliquots of the cell suspension described above in microtitre plates (clear-bottom polypropylene 96-well plates; Nunc A/S, Roskilde, Denmark), and incubating them at 30°C with 2 min of orbital shaking every 15 min. Bacterial growth was estimated by periodically monitoring the OD<sub>600</sub> in either a SpectraMax Plus<sup>384</sup> microplate reader (Molecular Devices, Sunnyvale, CA, USA) or a Wallac VICTOR<sup>2</sup><sup>TM</sup> 1420 multi-label counter and microplate reader (PerkinElmer, Waltham, MA, USA). Results of turbidity measurements were computed during exponential growth, and the specific growth rate (µ) was calculated for each condition as  $\mu = [\ln(\text{OD}_{600} \text{ at } t_1) - \ln(\text{OD}_{600} \text{ at } t_0)] / (t_1 - t_0)$ . For some experiments, growth retardation (i.e. extension of the lag phase) was analytically obtained as described by Dalggaard and Koutsoumanis

(2001). Normalized growth coefficients were calculated as  $100 \times (\mu_{\text{experimental}}/\mu_{\text{control}})$ , where  $\mu_{\text{experimental}}$  and  $\mu_{\text{control}}$  are the specific growth rates under stressful and control (i.e. in the absence of the stressor) growth conditions respectively. Soft-agar assays for determination of the cells' sensitivity to oxidative stress were carried out as described elsewhere (Sternberg and Maurer, 1991). In some experiments, oxidative stress conditions were imposed by adding DA [1,1'-azo-bis(*N,N*-dimethylformamide)] to the cultures from a concentrated solution freshly prepared in dimethylsulphoxide, and an appropriate volume of dimethylsulphoxide was added to control cultures. DA solutions were routinely titrated to ensure reproducible additions of the compound using an extinction coefficient ( $\epsilon_{\text{DA}}$ ) of  $3.02 \text{ mM}^{-1} \text{ cm}^{-1}$  (Kosower and Kosower, 1995). In soft-agar assays,  $\text{H}_2\text{O}_2$  was directly added from a 30% (v/v) stock solution (Sigma-Aldrich, St. Louis, MO, USA) to filter discs placed onto the homogeneous bacterial lawn. L-methionine stock solutions were freshly prepared in milli-Q water, and used at a final concentration of  $50 \mu\text{g ml}^{-1}$ .

#### *pfkA*<sup>E. coli</sup> expression tests and enzymatic assays

Cultures of *P. putida* (pVLT31) and *P. putida* (pVLT31-*pfkA*) were grown on LB medium containing  $10 \mu\text{g ml}^{-1}$  tetracycline and 0.5 mM IPTG until exponential growth phase ( $\text{OD}_{600} \sim 0.5\text{--}0.6$ ). *PfkA*<sup>E. coli</sup> expression was monitored in SDS-PAGE under denaturing conditions as follows: cells were harvested by centrifugation (2 min, 14 000 g, room temperature) such that a cell mass equivalent of 1 ml of culture at an  $\text{OD}_{600} = 1$  was adjusted to disperse in 200  $\mu\text{l}$  of denaturing loading buffer [63 mM Tris-HCl, 10% (v/v) glycerol, 2% (w/v) SDS, 2% (v/v) 2-mercaptoethanol, 0.0025% (w/v) bromophenol blue (pH = 6.8)] and heated at 100°C for 5 min. Aliquots of the cell lysates (10  $\mu\text{l}$ ) were directly loaded into the wells of a denaturing SDS-PAGE system containing 10% (w/v) polyacrylamide (Laemmli, 1970), and stained with Coomassie Brilliant Blue to visualize the corresponding protein bands (Sambrook and Russell, 2001).

For *in vitro* determinations of *PfkA*<sup>E. coli</sup> activity, cell-free extracts of *P. putida* (pVLT31) used as negative control, *E. coli* W3110 (positive control) and *P. putida* (pVLT31-*pfkA*) were prepared from pellets of 50 ml of culture aliquots. Cultures were developed as detailed above, harvested in the exponential growth phase ( $\text{OD}_{600} \sim 0.5\text{--}0.6$ ) by centrifugation (15 min, 4000 g, 4°C) and the pellets resuspended in 50 mM phosphate buffer (pH = 7.5), such that a cell mass equivalent of 50 ml of culture at an  $\text{OD}_{600} = 0.6$  was adjusted to disperse in 2 ml of buffer. Afterwards, cells were lysed by sonication in the cold (five pulses of 30 s each) and spun down (30 min, 14 000 g, 4°C) to collect cell debris. The supernatant was used for protein determinations (Bradford, 1976) and enzymatic assays of PFK activity were conducted essentially according to the protocol described by Steinbüchel (1986). Briefly, the PFK activity was determined in a reaction mixture (200  $\mu\text{l}$ ) containing 100 mM Tris-HCl (pH = 8.2), 10 mM  $\text{MgCl}_2$ , 2 mM  $\text{NH}_4\text{Cl}$ , 1 mM F6P, 0.2 mM NADH, 1 U  $\text{ml}^{-1}$  of fructose-1,6-bisphosphate aldolase, 3 U  $\text{ml}^{-1}$  of triosephosphate isomerase, 1 U  $\text{ml}^{-1}$  of glycerol-3-phosphate dehydrogenase and an adequate volume of cell-free extract corresponding to 20  $\mu\text{g}$  of total protein. All the enzymes used

in the assay were from *Saccharomyces cerevisiae* (Sigma-Aldrich). The reaction was started by the addition of 1 mM ATP, and NADH oxidation was monitored by continuously following the decrease in absorbance at 340 nm and 25°C during 5 min in microtitre plates as detailed above. Specific PFK activities were calculated using an extinction coefficient ( $\epsilon_{\text{NADH}}$ ) of  $6.22 \text{ mM}^{-1} \text{ cm}^{-1}$ . One unit of PFK activity was defined as the quantity of enzyme that catalysed the formation of 1  $\mu\text{mol}$  of  $\text{NAD}^+$  during 1 min at 25°C.

#### Determination of the ATP content and redox status of the cells

Pre-cultures of *P. putida* (pVLT31) and *P. putida* (pVLT31-*pfkA*) were diluted to an  $\text{OD}_{600}$  of  $\sim 0.1$  in M9 minimal medium containing 10 mM glucose and  $10 \mu\text{g ml}^{-1}$  tetracycline, and incubated at 30°C for 3 h. At that point, expression of *pfkA*<sup>E. coli</sup> was induced by adding 0.5 mM IPTG and cultures were further grown for 2 h. Then, cells were rapidly cooled on an ice bath and immediately used for *in vitro* determinations. ATP was measured using a commercially available ATP bioluminescence kit (Biaffin, Kassel, Germany). ATP was extracted from the cells according to the trichloroacetic acid protocol (Bagnara and Finch, 1972) as follows: 1 ml of cell culture was centrifuged (1 min, 14 000 g, 4°C) and the cell pellet resuspended in 250  $\mu\text{l}$  of ice-cold 50 mM phosphate buffer (pH = 7.5), added with 250  $\mu\text{l}$  of 5% (w/v) trichloroacetic acid containing 4 mM EDTA and cooled in an ice bath for 15 min (Lundin and Thore, 1975). Samples were diluted 20-fold with 20 mM Tris-HCl containing 2 mM EDTA (pH = 7.75), and 50  $\mu\text{l}$  of this solution was mixed with 50  $\mu\text{l}$  of the bioluminescence reagent supplied along with the kit according to the manufacturer's instructions. The bioluminescence signal was measured in a Wallac VICTOR<sup>2</sup>™ 1420 multi-label counter and microplate reader and then analysed by means of the WorkOut<sup>™</sup> applications data analysis software (Wallac Oy, Turku, Finland). Cell dry weight was determined from valorated culture aliquots as described elsewhere (Nikel *et al.*, 2008a). Intracellular levels of pyridine nucleotide cofactors were estimated by using *in vitro* procedures based on rapid inactivation of the metabolism of growing cells followed by acid or alkaline nucleotide extraction (Bernofsky and Swan, 1973; Nikel *et al.*, 2008b), with some modifications. Cells were collected by centrifugation (2 min, 8500 g, 4°C) and the pellets were rapidly washed once with ice-cold 50 mM phosphate buffer (pH = 7.5). After resuspending the biomass, 300  $\mu\text{l}$  of either 0.25 M NaOH [for NAD(P)H extraction] or HCl [for NAD(P)<sup>+</sup> extraction] was added to the cell suspension, which was then heated for 10 min at 55°C. Extracts were neutralized by dropwise addition of 300  $\mu\text{l}$  of 0.1 M HCl [for NAD(P)H extraction] or NaOH [for NAD(P)<sup>+</sup> extraction]. Cellular debris was removed by centrifugation (5 min, 12 000 g, room temperature), and supernatants were transferred to new tubes and stored at -20°C for no longer than 24 h. Cyclic assays for nucleotide determinations were conducted by aliquoting either 50  $\mu\text{l}$  of the oxidized sample and 50  $\mu\text{l}$  of 0.1 M NaCl or 100  $\mu\text{l}$  of the reduced sample in a single well in 96-well microtitre plates containing the reaction mixture. The components in the assay mixture and their final concentrations were 450 mM

bicine-NaOH (pH = 8.0), 2.5 mM 3-[4,5-dimethylthiazole-2-yl]-2,5-diphenyltetrazolium bromide (MTT), 15 mM EDTA, 1.5 mM phenazine ethosulfate and the cognate substrate (either 1.25 M ethanol or 12.5 mM G6P). After addition of the appropriate reaction mixture (i.e. containing ethanol for NAD determinations and G6P for NADP determinations), the plate was incubated at 30°C for 5 min in the dark. Reactions were started by prompt addition of either 10 U ml<sup>-1</sup> of alcohol dehydrogenase (ADHII) or 0.25 U ml<sup>-1</sup> of G6P dehydrogenase. These enzymes were from *S. cerevisiae* (Sigma-Aldrich). The formation of reduced MTT was continuously monitored at 570 nm and 30°C using a SpectraMax Plus<sup>384</sup> microplate reader. Cofactor concentration in each sample was determined from a calibration curve generated with authentic standards (Sigma-Aldrich) included on the same assay plate, and referred to the amount of biomass used to extract the nucleotides. The intracellular nucleotides concentration was determined as described elsewhere (Fuhrer and Sauer, 2009). The total redox ratio was defined as  $([NADH] + [NADPH])/([NAD^+] + [NADP^+])$ .

### Acknowledgements

The authors are indebted to A. Danchin for illuminating hints on the connection between methionine biosynthesis and NADPH demand, and to H. J. Ruijsenaars and L. M. Blank for their helpful suggestions. We are also indebted to J. Tamames for his help in phylogenetic analysis of PFK. This study was supported by the BIO and FEDER CONSOLIDER-INGENIO programme of the Spanish Ministry of Science and Innovation, the MICROME and ST-FLOW Contracts of the EU, the ERANET Program, and the PROMT Project of the CAM. M. C. was the recipient of a fellowship from the University of Costa Rica. P. I. N. is a researcher from the Consejo Nacional de Investigaciones Científicas y Técnicas (Argentina) and holds an EMBO Long-Term Fellowship (ALTF 13-2010). D. P. P. is a beneficiaria of a Marie Curie grant of the EC for visiting scholars. The authors declare no conflicts of interest.

### References

- Baart, G.J.E., Langenhof, M., van de Waterbeemd, B., Hamstra, H.J., Zomer, B., van der Pol, L.A., *et al.* (2010) Expression of phosphofructokinase in *Neisseria meningitidis*. *Microbiology* **156**: 530–542.
- Bagdasarian, M., Lurz, R., Rückert, B., Franklin, F.C.H., Bagdasarian, M.M., Frey, J., and Timmis, K.N. (1981) Specific purpose plasmid cloning vectors. II. Broad host range, high copy number, RSF1010-derived vectors, and a host-vector system for gene cloning in *Pseudomonas*. *Gene* **16**: 237–247.
- Bagnara, A.S., and Finch, L.R. (1972) Quantitative extraction and estimation of intracellular nucleoside triphosphates of *Escherichia coli*. *Anal Biochem* **45**: 24–34.
- Bar-Even, A., Flamholz, A., Noor, E., and Milo, R. (2012) Rethinking glycolysis: on the biochemical logic of metabolic pathways. *Nat Chem Biol* **8**: 509–517.
- Bearson, B.L., Lee, I.S., and Casey, T.A. (2009) *Escherichia coli* O157:H7 glutamate- and arginine-dependent acid-resistance systems protect against oxidative stress during extreme acid challenge. *Microbiology* **155**: 805–812.
- Benov, L., Kredich, N.M., and Fridovich, I. (1996) The mechanism of the auxotrophy for sulfur-containing amino acids imposed upon *Escherichia coli* by superoxide. *J Biol Chem* **271**: 21037–21040.
- Bernofsky, C., and Swan, M. (1973) An improved cycling assay for nicotinamide adenine dinucleotide. *Anal Biochem* **53**: 452–458.
- Blank, L.M., Ionidis, G., Ebert, B.E., Bühler, B., and Schmid, A. (2008) Metabolic response of *Pseudomonas putida* during redox biocatalysis in the presence of a second octanol phase. *FEBS J* **275**: 5173–5190.
- Blank, L.M., Ebert, B.E., Buehler, K., and Bühler, B. (2010) Redox biocatalysis and metabolism: molecular mechanisms and metabolic network analysis. *Antioxid Redox Signal* **13**: 349–394.
- Bradford, M.M. (1976) A rapid and sensitive method for the quantitation of microgram quantities of protein utilizing the principle of protein-dye binding. *Anal Biochem* **72**: 248–254.
- Butler, M.J., Bruheim, P., Jovetic, S., Marinelli, F., Postma, P.W., and Bibb, M.J. (2002) Engineering of primary carbon metabolism for improved antibiotic production in *Streptomyces lividans*. *Appl Environ Microbiol* **68**: 4731–4739.
- Carmel-Harel, O., and Storz, G. (2000) Roles of the glutathione- and thioredoxin-dependent reduction systems in the *Escherichia coli* and *Saccharomyces cerevisiae* responses to oxidative stress. *Annu Rev Microbiol* **54**: 439–461.
- del Castillo, T., Ramos, J.L., Rodríguez-Herva, J.J., Fuhrer, T., Sauer, U., and Duque, E. (2007) Convergent peripheral pathways catalyze initial glucose catabolism in *Pseudomonas putida*: genomic and flux analysis. *J Bacteriol* **189**: 5142–5152.
- Chavarría, M., Santiago, C., Platero, R., Krell, T., Casasnovas, J.M., and de Lorenzo, V. (2011) Fructose 1-phosphate is the preferred effector of the metabolic regulator Cra of *Pseudomonas putida*. *J Biol Chem* **286**: 9351–9359.
- Chavarría, M., Kleijn, R.J., Sauer, U., Pflüger-Grau, K., and de Lorenzo, V. (2012a) Regulatory tasks of the phosphoenolpyruvate-phosphotransferase system of *Pseudomonas putida* in central carbon metabolism. *mBio* **3**: e00028–e00012.
- Chavarría, M., Fuhrer, T., Sauer, U., Pflüger-Grau, K., and de Lorenzo, V. (2012b) Cra regulates the cross-talk between the two branches of the phosphoenolpyruvate:phosphotransferase system of *Pseudomonas putida*. *Environ Microbiol* (In Press). DOI: 10.1111/j.1462-2920.2012.02808.x.
- Choi, K.H., Kumar, A., and Schweizer, H.P. (2006) A 10-min method for preparation of highly electrocompetent *Pseudomonas aeruginosa* cells: application for DNA fragment transfer between chromosomes and plasmid transformation. *J Microbiol Methods* **64**: 391–397.
- Conway, T. (1992) The Entner–Doudoroff pathway: history, physiology and molecular biology. *FEMS Microbiol Rev* **9**: 1–27.
- Cumming, R.C., Andon, N.L., Haynes, P.A., Park, M., Fischer, W.H., and Schubert, D. (2004) Protein disulfide

- bond formation in the cytoplasm during oxidative stress. *J Biol Chem* **279**: 21749–21758.
- Dalgaard, P., and Koutsoumanis, K. (2001) Comparison of maximum specific growth rates and lag times estimated from absorbance and viable count data by different mathematical models. *J Microbiol Methods* **43**: 183–196.
- De Ley, J. (1960) Comparative carbohydrate metabolism and localization of enzymes in *Pseudomonas* and related micro-organisms. *J Appl Bacteriol* **23**: 400–441.
- Demple, B. (1991) Regulation of bacterial oxidative stress genes. *Annu Rev Genet* **25**: 315–337.
- Duque, E., Molina-Henares, A.J., Torre, J., Molina-Henares, M.A., del Castillo, T., Lam, J., and Ramos, J.L. (2007) Towards a genome-wide mutant library of *Pseudomonas putida* strain KT2440. In *Pseudomonas: A Model System in Biology*. Ramos, J.L., and Filloux, A. (eds). Berlin, Germany: Springer, pp. 227–251.
- Ebert, B.E., Kurth, F., Grund, M., Blank, L.M., and Schmid, A. (2011) Response of *Pseudomonas putida* KT2440 to increased NADH and ATP demand. *Appl Environ Microbiol* **77**: 6597–6605.
- Entner, N., and Doudoroff, M. (1952) Glucose and gluconic acid oxidation of *Pseudomonas saccharophila*. *J Biol Chem* **196**: 853–862.
- Fabris, M., Matthijs, M., Rombauts, S., Vyverman, W., Goossens, A., and Baart, G.J.E. (2012) The metabolic blueprint of *Phaeodactylum tricornutum* reveals a eukaryotic Entner–Doudoroff glycolytic pathway. *Plant J* **70**: 1004–1014.
- Fuchs, G., Boll, M., and Heider, J. (2011) Microbial degradation of aromatic compounds – from one strategy to four. *Nat Rev Microbiol* **9**: 803–816.
- Fuhrer, T., and Sauer, U. (2009) Different biochemical mechanisms ensure network-wide balancing of reducing equivalents in microbial metabolism. *J Bacteriol* **191**: 2112–2121.
- Fuhrer, T., Fischer, E., and Sauer, U. (2005) Experimental identification and quantification of glucose metabolism in seven bacterial species. *J Bacteriol* **187**: 1581–1590.
- Harada, E., Iida, K.I., Shiota, S., Nakayama, H., and Yoshida, S.I. (2010) Glucose metabolism in *Legionella pneumophila*: dependence on the Entner–Doudoroff pathway and connection with intracellular bacterial growth. *J Bacteriol* **192**: 2892–2899.
- Hofmann, E. (1976) The significance of phosphofructokinase to the regulation of carbohydrate metabolism. *Rev Physiol Biochem Pharmacol* **75**: 1–68.
- Hondorp, E.R., and Matthews, R.G. (2004) Oxidative stress inactivates cobalamin-independent methionine synthase (MetE) in *Escherichia coli*. *PLoS Biol* **2**: e336.
- Imlay, J.A. (2008) Cellular defenses against superoxide and hydrogen peroxide. *Annu Rev Biochem* **77**: 755–776.
- Izawa, S., Inoue, Y., and Kimura, A. (1996) Importance of catalase in the adaptive response to hydrogen peroxide: analysis of acatalasaemic *Saccharomyces cerevisiae*. *Biochem J* **320**: 61–67.
- Jang, S.G., Lee, B.M., and Cho, J.Y. (2012) Effect of modified glucose catabolism on xanthan production in *Xanthomonas oryzae* pv. *oryzae*. *J Ind Microbiol Biotechnol* **39**: 649–654.
- Kim, J., and Copley, S.D. (2007) Why metabolic enzymes are essential or nonessential for growth of *Escherichia coli* K12 on glucose. *Biochemistry* **46**: 12501–12511.
- Kim, J., Jeon, C.O., and Park, W. (2008) Dual regulation of *zwf-1* by both 2-keto-3-deoxy-6-phosphogluconate and oxidative stress in *Pseudomonas putida*. *Microbiology* **154**: 3905–3916.
- Kosower, N.S., and Kosower, E.M. (1995) Diamide: an oxidant probe for thiols. *Methods Enzymol* **251**: 123–133.
- Laemmli, U.K. (1970) Cleavage of structural proteins during the assembly of the head of bacteriophage T4. *Nature* **227**: 680–685.
- Latour, X., and Lemanceau, P. (1997) Métabolisme carboné et énergétique des *Pseudomonas* spp fluorescents saprophytes à oxydase positive. *Agronomie* **17**: 427–443.
- de Lorenzo, V., Eltis, L., Kessler, B., and Timmis, K.N. (1993) Analysis of *Pseudomonas* gene products using *lacI/P<sub>trp</sub>-lac* plasmids and transposons that confer conditional phenotypes. *Gene* **123**: 17–24.
- Loza-Tavera, H., and de Lorenzo, V. (2011) Microbial bioremediation of chemical pollutants: how bacteria cope with multi-stress environmental scenarios. In *Bacterial Stress Responses*. Storz, G., and Hengge, R. (eds). Washington, DC, USA: ASM Press, pp. 481–492.
- Lundin, A., and Thore, A. (1975) Comparison of methods for extraction of bacterial adenine nucleotides determined by firefly assay. *Appl Microbiol* **30**: 713–721.
- Meijnen, J.P., de Winde, J.H., and Ruijsenaars, H.J. (2012) Metabolic and regulatory rearrangements underlying efficient D-xylose utilization in engineered *Pseudomonas putida* S12. *J Biol Chem* **287**: 14606–14614.
- Miller, J.H. (1972) *Experiments in Molecular Genetics*. Cold Spring Harbor, NY, USA: Cold Spring Harbor Laboratory.
- Molina-Henares, M.A., Torre, J., García-Salamanca, A., Molina-Henares, A.J., Herrera, M.C., Ramos, J.L., and Duque, E. (2010) Identification of conditionally essential genes for growth of *Pseudomonas putida* KT2440 on minimal medium through the screening of a genome-wide mutant library. *Environ Microbiol* **12**: 1468–1485.
- Neidhardt, F.C., Ingraham, J.L., and Schaechter, M. (1990) *Physiology of the Bacterial Cell: A Molecular Approach*. Sunderland, MA, USA: Sinauer Associates.
- Nelson, K.E., Weinl, C., Paulsen, I.T., Dodson, R.J., Hilbert, H., Martins dos Santos, V.A.P., et al. (2002) Complete genome sequence and comparative analysis of the metabolically versatile *Pseudomonas putida* KT2440. *Environ Microbiol* **4**: 799–808.
- Nikel, P.I., Pettinari, M.J., Galvagno, M.A., and Méndez, B.S. (2008a) Poly(3-hydroxybutyrate) synthesis from glycerol by a recombinant *Escherichia coli* *arcA* mutant in fed-batch microaerobic cultures. *Appl Microbiol Biotechnol* **77**: 1337–1343.
- Nikel, P.I., Pettinari, M.J., Ramirez, M.C., Galvagno, M.A., and Méndez, B.S. (2008b) *Escherichia coli* *arcA* mutants: metabolic profile characterization of microaerobic cultures using glycerol as a carbon source. *J Mol Microbiol Biotechnol* **15**: 48–54.
- Nogales, J., Palsson, B., and Thiele, I. (2008) A genome-scale metabolic reconstruction of *Pseudomonas putida* KT2440: iJN746 as a cell factory. *BMC Syst Biol* **2**: 79.
- Patra, T., Koley, H., Ramamurthy, T., Ghose, A.C., and

- Nandy, R.K. (2012) The Entner–Doudoroff pathway is obligatory for gluconate utilization and contributes to the pathogenicity of *Vibrio cholerae*. *J Bacteriol* **194**: 3377–3385.
- Peekhaus, N., and Conway, T. (1998) What's for dinner?: Entner–Doudoroff metabolism in *Escherichia coli*. *J Bacteriol* **180**: 3495–3502.
- Pérez-Pantoja, D., Donoso, R., Agulló, L., Córdova, M., Seeger, M., Pieper, D.H., and González, B. (2012) Genomic analysis of the potential for aromatic compounds biodegradation in *Burkholderiales*. *Environ Microbiol* **14**: 1091–1117.
- Pöther, D.C., Liebecke, M., Hochgräfe, F., Antelmann, H., Becher, D., Lalk, M., *et al.* (2009) Diamide triggers mainly S thiolations in the cytoplasmic proteomes of *Bacillus subtilis* and *Staphylococcus aureus*. *J Bacteriol* **191**: 7520–7530.
- Puchařka, J., Oberhardt, M.A., Godinho, M., Bielecka, A., Regenhardt, D., Timmis, K.N., *et al.* (2008) Genome-scale reconstruction and analysis of the *Pseudomonas putida* KT2440 metabolic network facilitates applications in biotechnology. *PLoS Comput Biol* **4**: e1000210.
- Ramos, J.L., Krell, T., Daniels, C., Segura, A., and Duque, E. (2009) Responses of *Pseudomonas* to small toxic molecules by a mosaic of domains. *Curr Opin Microbiol* **12**: 215–220.
- Ravasz, E., Somera, A.L., Mongru, D.A., Oltvai, Z.N., and Barabási, A.L. (2002) Hierarchical organization of modularity in metabolic networks. *Science* **297**: 1551–1555.
- Richhardt, J., Bringer, S., and Bott, M. (2012) Mutational analysis of the pentose phosphate and Entner–Doudoroff pathways in *Gluconobacter oxydans* reveals improved growth of a  $\Delta edd \Delta eda$  mutant on mannitol. *Appl Environ Microbiol* **78**: 6975–6986.
- Romano, A.H., and Conway, T. (1996) Evolution of carbohydrate metabolic pathways. *Res Microbiol* **147**: 448–455.
- Ronimus, R.S., and Morgan, H.W. (2001) The biochemical properties and phylogenies of phosphofructokinases from extremophiles. *Extremophiles* **5**: 357–373.
- Sambrook, J., and Russell, D.W. (2001) *Molecular Cloning: A Laboratory Manual*. Cold Spring Harbor, NY, USA: Cold Spring Harbor Laboratory.
- Sato, T., and Atomi, H. (2011) Novel metabolic pathways in Archaea. *Curr Opin Microbiol* **14**: 307–314.
- Sawyer, M.H., Baumann, P., Baumann, L., Berman, S.M., Cánovas, J.L., and Berman, R.H. (1977) Pathways of D-fructose catabolism in species of *Pseudomonas*. *Arch Microbiol* **112**: 49–55.
- Schleissner, C., Reglero, A., and Luengo, J.M. (1997) Catabolism of D-glucose by *Pseudomonas putida* U occurs via extracellular transformation into D-gluconic acid and induction of a specific gluconate transport system. *Microbiology* **143**: 1595–1603.
- Sekowska, A., Kung, H.F., and Danchin, A. (2000) Sulfur metabolism in *Escherichia coli* and related bacteria: facts and fiction. *J Mol Microbiol Biotechnol* **2**: 145–177.
- Singh, R., Mailloux, R.J., Puiseux-Dao, S., and Appanna, V.D. (2007) Oxidative stress evokes a metabolic adaptation that favors increased NADPH synthesis and decreased NADH production in *Pseudomonas fluorescens*. *J Bacteriol* **189**: 6665–6675.
- Sohn, S.B., Kim, T.Y., Park, J.M., and Lee, S.Y. (2010) *In silico* genome-scale metabolic analysis of *Pseudomonas putida* KT2440 for polyhydroxyalkanoate synthesis, degradation of aromatics and anaerobic survival. *Biotechnol J* **5**: 739–750.
- Sprenger, G.A. (1995) Genetics of pentose-phosphate pathway enzymes of *Escherichia coli* K-12. *Arch Microbiol* **164**: 324–330.
- Steinbüchel, A. (1986) Expression of the *Escherichia coli* *pfkA* gene in *Alcaligenes eutrophus* and in other Gram-negative bacteria. *J Bacteriol* **166**: 319–327.
- Sternberg, N.L., and Maurer, R. (1991) Bacteriophage-mediated generalized transduction in *Escherichia coli* and *Salmonella typhimurium*. *Methods Enzymol* **204**: 18–43.
- Storz, G., and Imlay, J.A. (1999) Oxidative stress. *Curr Opin Microbiol* **2**: 188–194.
- Storz, G., Tartaglia, L.A., Farr, S.B., and Ames, B.N. (1990) Bacterial defenses against oxidative stress. *Trends Genet* **6**: 363–368.
- Velázquez, F., di Bartolo, I., and de Lorenzo, V. (2004) Genetic evidence that catabolites of the Entner–Doudoroff pathway signal C source repression of the  $\sigma^{54}$  *Pu* promoter of *Pseudomonas putida*. *J Bacteriol* **186**: 8267–8275.
- Vicente, M., and Cánovas, J.L. (1973a) Glucolysis in *Pseudomonas putida*: physiological role of alternative routes from the analysis of defective mutants. *J Bacteriol* **116**: 908–914.
- Vicente, M., and Cánovas, J.L. (1973b) Regulation of the glycolytic enzymes in *Pseudomonas putida*. *Arch Microbiol* **93**: 53–64.
- Wax, R., Rosenberg, E., Kosower, N.S., and Kosower, E.M. (1970) Effect of the thiol-oxidizing agent diamide on the growth of *Escherichia coli*. *J Bacteriol* **101**: 1092–1093.
- Ying, W. (2008) NAD<sup>+</sup>/NADH and NADP<sup>+</sup>/NADPH in cellular functions and cell death: regulation and biological consequences. *Antioxid Redox Signal* **10**: 179–206.

### Supporting information

Additional Supporting Information may be found in the online version of this article:

Supplementary experimental procedures.

**Fig. S1.** Phylogenetic profiling of 6-phosphofructokinases in bacteria. Phylogenetic profiling reveals that many genomes of  $\gamma$ -proteobacteria, firmicutes, bacteroidetes, *Acidobacterium* and some cyanobacteria contain either a *pfkA* or *pfkB* gene, while it is absent in most  $\alpha$ -proteobacteria,  $\beta$ -proteobacteria and Chlamydiae genomes. Furthermore, phylogenetic profiling indicates that *pfk* genes are usually absent in the genomes of most aerobic microorganisms (e.g. *Pseudomonas* species), while most anaerobic or facultative anaerobic organisms contain a *pfkA* gene. Since little energy is generated from C substrates in strict anaerobic species, the relative gain in ATP yield increases significantly when 6-phosphofructokinase (i.e. a complete Embden–Meyerhof–Parnas glycolytic pathway) is present.

**Fig. S2.** Scheme of the pathways involved in glucose catabolism in *Pseudomonas putida* KT2440. After the initial phosphorylation of glucose, catalysed by glucokinase (Gik), the resulting glucose-6-P is channelled through the Entner–

Doudoroff pathway (Edd/Eda) via its conversion into 6-*P*-gluconate and 6-*P*-2-keto-3-deoxygluconate to finally yield pyruvate and glyceraldehyde-3-*P*. Glucose can also be converted into gluconate, 2-ketogluconate and 6-*P*-2-ketogluconate in the so-called gluconate and 2-ketogluconate loops but these intermediates are ultimately converted into 6-*P*-gluconate and yield the same C3 compounds as mentioned above. Pyruvate is transformed into acetyl-coenzyme A (CoA) through the activity of the pyruvate dehydrogenase complex (AceEF and other components, as depicted) in a NAD<sup>+</sup>-dependent reaction. Although acetyl-CoA can meet different fates depending on further catabolic steps, it is mainly oxidized in the tricarboxylic acid cycle. The reducing equivalents therein produced as NADH are used as electron donors in the respiratory chain, thereby generating

ATP during the oxidative phosphorylation process. The relevant enzymatic steps are identified in parentheses by means of their locus (PP) numbers as annotated by Nelson and colleagues (2002). *P*, inorganic phosphate; PQQ, pyrroloquinoline quinone.

**Fig. S3.** Sensitivity of *E. coli* MG1655, *A. tumefaciens* C58C1, *P. putida* KT2440 and *P. aeruginosa* PAO1 to oxidative stress imposed by diamide. The resistance to diamide depends on NADPH-dependent thioredoxins, so that the response of the bacteria to the stress generated by this compound ultimately depends on the intracellular redox state. As it can be seen in the inhibition halos for each species, *P. putida* and *P. aeruginosa* present a higher tolerance to diamide than *E. coli* and *A. tumefaciens*.

**Table S1.** Bacterial strains and plasmids used in this work.